Physics of the Earth and Planetary Interiors, 67 (1991) 48–64
Elsevier Science Publishers B.V., Amsterdam

Frequency dependence and spatial distribution of seismic attenuation in France: experimental results and possible interpretations

M. Campillo [1] and J.L. Plantet [2]

[1] *Laboratoire de Géophysique Interne et Tectonophysique, Université Joseph Fourier, and Observatoire de Grenoble IRIGM, B.P. 53X, 38041 Grenoble (France)*

[2] *Laboratoire de Détection Géophysique, Commissariat à l'Energie Atomique, B.P. 12, 91680 Bruyère-le-Chatel (France)*

(Received 3 December 1989; revision accepted 15 May 1990)

ABSTRACT

Campillo, M. and Plantet, J.L., 1991. Frequency dependence and spatial distribution of seismic attenuation in France: experimental results and possible interpretations. Phys. Earth Planet. Inter., 67: 48–64.

We processed digital records from 431 earthquakes at 25 stations of the Laboratoire de Détection Géophysique network in France. We computed spectral amplitudes of Pg and Lg in different group velocity windows. This large data set allowed us to compute a map of mean crustal attenuation through simultaneous consideration of source amplitude, site response and apparent Q. Our inversion procedure combines an iterative reconstruction technique with an adjustment of source amplitudes and site responses at each step. The stability of the result is tested with different subsets of data and the resolution is evaluated. Maps of apparent attenuation at frequencies between 1.5 and 10 Hz were computed from Pg, Lg and early coda of Lg.

These results are in a good agreement with the predictions of the single-scattering model both for frequency dependence and for $Q_s : Q_p$ ratios. The comparison between the attenuation anomaly found in the Variscan belt and results from a deep reflection seismic profile confirms the prominent part played by scattering in the apparent attenuation of seismic waves in the crust.

1. Introduction

The short-period seismic phases Pg and Lg have been extensively studied for the purposes of nuclear test monitoring, magnitude determination or attenuation measurements (e.g. Nuttli, 1973, 1986). Considering regions in which a flat layering can be regarded as a reasonable model for the Earth's crust, the mode of propagation of these phases has been clearly established by comparison between its observed and theoretical properties. The theoretical results have been obtained using oversimplified models of the crust which consist of stacks of a few flat visco-elastic layers, each of them being considered as homogeneous at any scale. Nevertheless, these numerical simulations fail to explain several very general features of regional phases. For instance, the long duration of the signals (the existence of a coda) in most of the observations is not accounted for. On the other hand, to explain the actual attenuation of these signals, it is necessary to include in the models a frequency-dependent quality factor that is not compatible with accepted processes of anelastic attenuation at depth (Johnston, 1981). These phenomena are generally attributed to scattering

0031-9201/91/$03.50

caused by imprecisely defined heterogeneities that have to be added to the vertical layering usually hypothesized. To describe crustal heterogeneity, we accept that it can be separated into small-scale and large-scale heterogeneities. The small-scale heterogeneity consists of the fluctuations of elastic properties at a scale roughly equal to or smaller than the wavelengths considered in short-period seismology. These fluctuations cannot be described from a deterministic point of view because the details of the crustal structure are far beyond our present knowledge. The implications of this type of heterogeneity have been studied in detail, particularly to explain the coda of local seismograms and the frequency dependence of the apparent attenuation (e.g. Sato, 1990). Since the pioneering work of Aki (1969), it is now clearly established that scattering on small fluctuations of elastic parameters can account, at least partially, for the existence of coda and for the frequency dependence of the apparent attenuation (Herraiz and Espinoza, 1987, review). Most of the developments of the theory of coda waves concern the perturbations of a homogeneous medium. This represents a severe limitation to the interpretation, as the Earth presents strong vertical heterogeneity. The importance of the layering for scattered waves was investigated by Wang and Herrmann (1988). The most obvious effect of stratification on the scattered field is the generation of surface waves.

Large-scale shallow irregularities such as sedimentary basins also produce local conversion of body waves into propagating surface waves (Campillo, 1987). Nevertheless, because of the large observed attenuation near the surface (Toksöz et al., 1988) and the great variability of the thickness of the surface low-velocity layer, we expect the short-period surface waves to be unable to propagate along paths of several hundreds of kilometers as Pg or Lg do. Various authors have tried to infer numerically the effect of deep irregularities, such as Moho uplifts, on short-period Lg (Kennett, 1984; Campillo, 1987; Maupin, 1989). Their basic conclusion is that Lg appears to be a robust and stable phase even when strong lateral variations of the crustal structure occur. In view of this result, the Lg wavetrain could be used to measure the mean attenuation in the crust. However, a single measure of the apparent attenuation does not give much information on the cause and the mechanism of seismic attenuation. A better approach would be to correlate the characteristics of attenuation in different regions with the various crustal structures encountered.

In this work, we follow such an approach. To avoid spurious differences that can be produced when comparing measurements made with different types of data or techniques, we used an inversion process and a relatively large homogeneous data set. To this end, we have to collect sufficient data to be able to describe attenuation in both space and frequency domains beneath an area large enough to include different geological units. Such is the case if we attempt to map the attenuation beneath France. In Fig. 1, the basic geological setting of France is displayed. The Paleozoic basement (Armorican and Central Massif), Mesozoic and Cenozoic basins (such as the Paris Basin) and the Alpine zone are shown in the figure. One must note that the Central Massif presents extension structures that developed during the Alpine orogenesis and that are part of the peri-alpine graben system.

We have obtained a large number of seismograms from the seismic network run by Laboratoire de Détection Géophysique (LDG) in France. This data set is sufficient to cover a great part of France. We require unclipped seismograms showing an acceptable signal-to-noise ratio in the epicentral distance range 200–1000 km. Because of the dynamic range of the network and the modest seismicity of France this represents a long observation time. In a previous study (Campillo, 1987), we used a limited number of earthquakes (18) and of stations (22) to study a region of central France. Because of the small number of records then available, we applied the back-projection technique to construct a map of apparent attenuation. We shall discuss these results below. In this study, we have widely increased the data set and the area studied. We will use an iterative SIRT-type reconstruction technique to determine source amplitude and quality factors. We also consider early coda of Lg and Pg waves. A related approach is that followed by Gupta et al. (1989) to study the distribution of Q from Lg in eastern

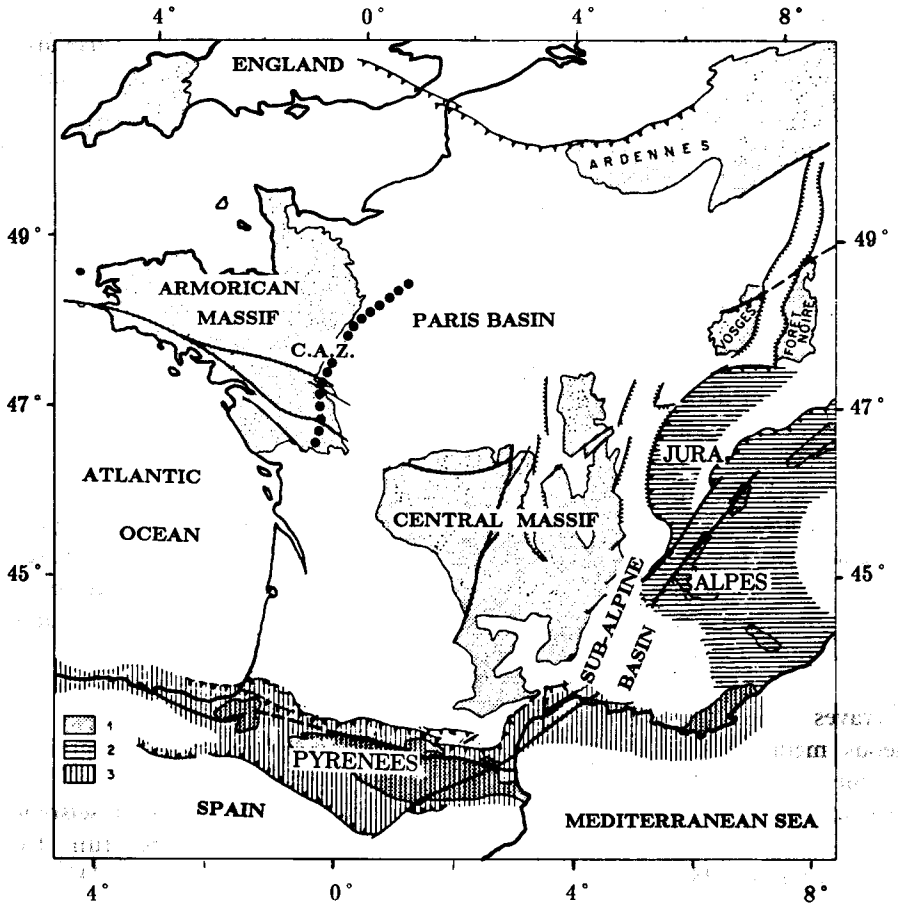

Fig. 1. Geological sketch map showing the main structural units in France. Stippled regions (1) indicate the Hercynian basement, and hatched regions (2 and 3) show the domain of the Alpine orogenesis. The black dots correspond to the part of the ECORS seismic line depicted in Fig. 11. This line crosses the Central Armorican zone (C.A.Z.). (Adapted from a map by A. Autran.)

North America. These authors assumed a regionalization based on Bouguer gravity contours and geological maps.

2. Data processing

We selected 431 earthquakes during the period 1985–1987 in France and in its vicinity (Fig. 2). These events were recorded at 26 short-period seismic stations of the LDG network. All stations are identical. Several examples of records have been shown by Nicolas et al. (1982) and by Campillo et al. (1985). The vertical seismometers have a natural frequency of 1 Hz, and the frequency band of the system ranges from 0.5 to 20 Hz. The network has been described by Nicolas et al. (1982). Unfortunately, we have never recorded simultaneously in good conditions at more than 20 stations. For each record, we computed the density of spectral amplitude for four phases defined by the group velocity windows:

$6.2\ \text{km s}^{-1} > V > 5.6\ \text{km s}^{-1}$ Pg

$3.6\ \text{km s}^{-1} > V > 3.1\ \text{km s}^{-1}$ Lg1

$3.1\ \text{km s}^{-1} > V > 2.6\ \text{km s}^{-1}$ Lg2

$2.6\ \text{km s}^{-1} > V > 2.3\ \text{km s}^{-1}$ Lg3

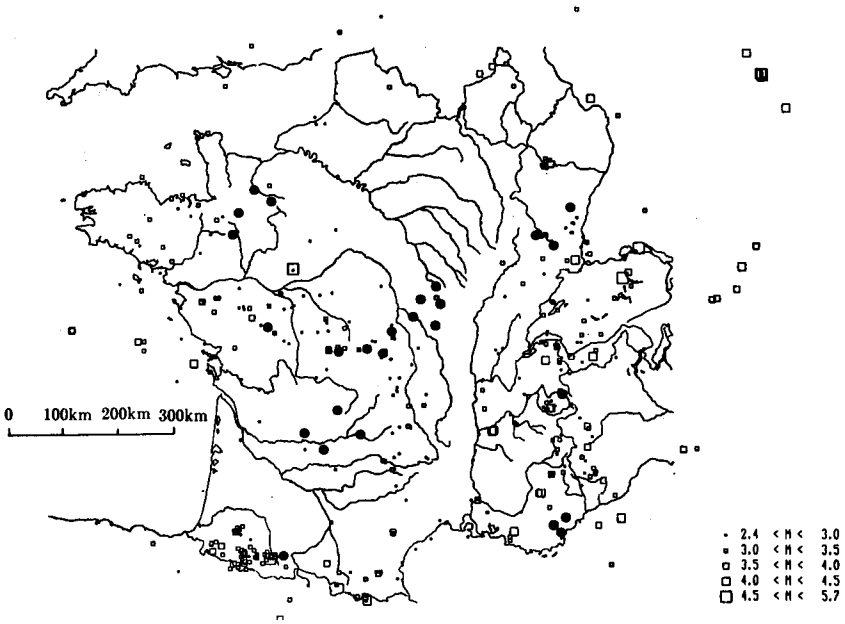

Fig. 2. Locations of earthquakes (squares) and stations (black dots) used in this study. All stations have exactly the same characteristics.

At this stage, we eliminated the traces where glitchs were detected. For each record, we also computed the density of spectral amplitude of the noise in a 30-s window before the first arrival. For a given phase and a given frequency, the spectral density is validated if the signal-to-noise ratio is greater than three.

3. Data analysis

We model the spectral amplitude observed at station i for earthquake j in the form

$$A_{i,j}(f, d) = S_j(f) \times E(d) \times AA_{i,j}(f, d) \times St_i(f) \quad (1)$$

where d represents the epicentral distance, f the frequency, S the source excitation, $E(d)$ the geometrical spreading, $AA_{i,j}(f, d)$ the apparent attenuation, and $St_i(f)$ is a term describing the site response at the station. For evaluation of the source excitation ($S_j(f)$) we neglect the radiation pattern due to the focal mechanism as well as the directivity effects associated with rupture propagation. The directivity is known to be a strong effect only on wavelengths much smaller than the source dimension. The Pg and Lg wavetrains are made up of arrivals corresponding to very different take-off angles and therefore the radiation pattern is, in general, very smoothed for these phases. The geometrical spreading of the phase considered in the time domain ($E(d)$) was found after numerical investigations in flat layered models (Campillo et al., 1984). Its functional dependence is given by

$$E(d) = d^{-0.83} \text{ for Lg} \quad (2)$$
$$E(d) = d^{-1.5} \text{ for Pg}$$

We assume in our analysis that Pg and Lg propagate mostly along straight ray paths, i.e. that the mean velocity of S waves in the crust is roughly constant. Therefore we neglect the effect of focusing–defocusing that was recognized for surface waves (e.g. Zeng et al., 1987).

For the apparent attenuation ($AA_{i,j}(f, d)$), we assume the form

$$AA_{i,j}(f, d) = \exp - \left[\frac{\pi f}{V} \int_d \frac{dl}{Q(f, x, y)} \right] \quad (3)$$

where V is the group velocity and Q is the quality factor. This term includes the intrinsic attenuation but also other types of attenuation such as scattering, or propagation effects in a heterogeneous crust that affect the geometrical spreading. The station response ($St_i(f)$) represents the amplification due to site effects at a given station. The azimuthal dependence of the site response is neglected. In a previous report (Campillo et al., 1985), we showed the importance of taking into account the site response of the station.

We performed our data analysis (and the inversion) independently for each frequency. The first step was to assume that the quality factor is constant over the area considered. We then evaluated the mean quality factor, the source excitation and the station response by an iterative process identical to the scheme used by Campillo et al. (1985). At first, we performed a linear regression to compute mean Q and S for each earthquake. When the correlation coefficient obtained is < 0.8, the event is eliminated. This value allows us to remove some erroneous data that were kept after our previous sorting, but it can also lead to exclusion of data corresponding to sharp propagation anomalies. We accept this risk because we believe that the anomalous zones are well known and are located outside our study zone, i.e. at oceanic margins or in the Italian Alps, where we observe that Lg waves completely disappear. To avoid wrong determinations of the source excitation, we use only the data for which the earthquake was recorded by at least five stations. An additional condition is that the difference of epicentral distance between the closest and the furthest station is $> 40\%$ of the largest epicentral distance.

The results obtained at this stage are used as a starting model for an iterative reconstruction that will be described in the next section. The mean values of Q_s that we obtain from Lg are very similar to our previous results (Campillo et al., 1985) and show the same frequency dependence (Q_s varies as the square-root of the frequency). Nevertheless, the fact that we are willing to cover a large area with a dense set of paths limits the frequency range available. The poor signal-to-noise ratio at low frequency means that we can work properly only with frequencies > 1 Hz. Figure 3 shows an example of the effective path coverage for a frequency of 3 Hz, after sorting out the data set.

Fig. 3. Path coverage at a frequency of 3 Hz after sorting of the raw data.

4. Algorithm of inversion

This algorithm is based on the use of an iterative reconstruction technique that allows us to consider large data sets on small computers. The general scheme of the complete processing is presented in Fig. 4. Stage I, as denoted in Fig. 4, was discussed in the last section and consists of setting up a starting model with a homogeneous $Q(f)$. In the next stage, we compute a set of Q values at the nodes of a regular grid to describe the actual continuous distribution of apparent attenuation.

After stage I we use eqn (1), the expression for the apparent attenuation, and the estimations of S and St to evaluate the parameter l_r for ray r:

$$l_r = \int_{d_r} \frac{\mathrm{d}l}{Q(f, x, y)}$$

The set of the l_r will be used to invert $Q(f, x, y)$.

The inversion techniques used are slightly modified versions of the back-projection and the simultaneous iterative reconstruction technique (SIRT). We shall briefly describe them.

Back-projection and SIRT operate for a given unknown $Q(f, x, y) = Q_i$ corresponding to location $X_i = (x, y)$ and with the data from the neighbouring paths. Following Mason (1981), we define a circle of influence around X_i. Each path contributes with a weighting coefficient proportional to its length within the circle of influence. This approach is particularly well suited to the present problem, as we know the important role played by scattered waves and multipathing in the propagation of regional phases. For the inversions presented in this study we used a grid mesh of 60 km and a radius of the circle of influence of 50 km. This means that the circles of influence overlap, which results in a smoothing of the results. An explicit smoothing was also performed at each step of the iterative inversion, as indicated in the following.

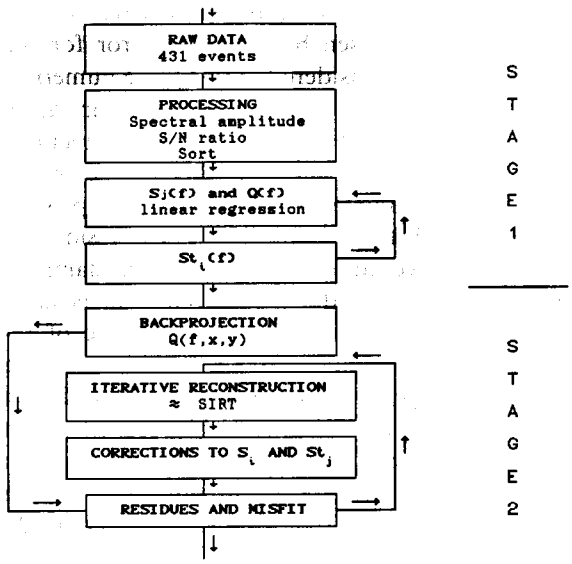

Fig. 4. Scheme of data processing and inversion.

The back-projection is then slightly modified by using the expression for a single-step local averaging:

$$Q_i^{-1} = \frac{\sum_{r=1}^{N_i} a_{r,i}(l_r/L_r)}{\sum_{r=1}^{N_i} a_{r,i}} \tag{4}$$

where N_i is the number of paths that cross the circle of influence centred on X_i, $a_{r,i}$ is the length of the path in the circle and L_r is its total length. We compute Q values at the locations X_i for which the number of rays is larger than $N_{\min}$. A supplementary condition is that these rays come from a number of distinct sources larger than $N_{S\min}$ When these conditions are not satisfied, the mean value of Q^{-1} is assumed. Without further precision, the results presented here are computed with $N_{\min} = 15$ and $N_{S\min} = 8$.

Following Cote (1988), we implemented an iterative inversion basically derived from SIRT (Gilbert, 1972). After the $(j-1)$th iteration we compute the estimation of the parameter l in the jth model: l_r^{j-1}. We define the residue by

$$\mathrm{res}_r^j = l_r - l_r^{j-1}$$

The jth iteration consists of applying to Q^{-1} at location X_i the correction

$$\delta\left(Q_i^{-1}\right)^j = \frac{\phi(e_i)}{e_i} \sum_{r=1}^{N_i} a_{r,i} g_i(\theta_r) \frac{\mathrm{res}_r^j}{L_r}$$

with

$$e_i = \sum_{r=1}^{N_i} a_{r,i} g_i(\theta_r) \qquad (5)$$

and where θ_r is the azimuth of the path r in degrees, and f and g are weighting functions which we are about to describe. $g(\theta_r)$ represents the azimuthal weighting:

$$g_i(\theta_r) = G + (1 - G)\left[N_i - D_i(\theta_r)\right]/N_i$$

where $D_i(\theta_r)$ is the number of paths whose directions are in the range $(\theta_r - 10°, \theta_r + 10°)$ and which intersect the circle of influence centered on X_i. G is a constant that controls the amplitude of the variation of the weighting and that we chose to be equal to 0.5. The effect of g is to moderate the influence of strong heterogeneities in the distribution of rays.

The damping factor $\phi(e_i)$ varies with the location and depends mainly on the density of rays:

$$\phi(e_i) = R + (1 - R) e_i / e_{\max}$$

where $e_{\max}$ is the maximum value of the sum of the weighting factors at each point computed over the entire region studied. R is a constant chosen to be equal to 0.5 in the following examples. By using a spatially dependent damping we want to limit the variations of the model in zones where the path coverage is poor. This is especially useful considering the uncertainties implied by our parametrization of the problem, as will be discussed in the next section. After each iteration we applied a smoothing filter defined by

$$\overline{Q}_i^{-1} = \frac{1}{2} Q_i^{-1} + \sum_{n=1}^{8} \frac{Q_n^{-1}}{16}$$

where $\overline{Q}_i^{-1}$ is the filtered value at location X_i, and the summation over n is extended to the eight neighbouring points around X_i in our square grid.

We have also performed tests where we added a constant to the weighting term e_i, as proposed by R.P. Comer and R.W. Clayton (unpublished manuscript, 1987), who suggested that this operation may stabilize the solution. In our case, this damping affects the convergence rate but has a very weak influence on the final image.

After a series of iterations to realize the current Q model, we compute the mean residues associated with each station and each earthquake. Next, the station responses and the source excitations are corrected by terms equal to these biases multiplied by damping factors. The values of these damping factors, relative to the mean damping applied for the inversion of Q alone, can be evaluated by comparing the partial derivatives of the amplitude with respect to Q_i, S and St in eqn. (1). In practice, the coefficients of damping for S and St, ϵ_S and ϵ_{St}, as well as the number of iterations on Q_i only, are chosen after numerous trials. We have studied systematically the influence of damping factors and number of internal iterations on the final misfits between model prediction and actual observations. With this aim, we repeated the inversion process tens of times with different parameters. We then chose the set of values that corresponds to the minimal final misfit (in the least-squares sense) after the convergence of the complete iterative process. In the following examples we have taken ϵ_S between 0.06 and 0.04, ϵ_{St} between 0.03 and 0.02, and the number of iterations of SIRT, on Q_i only, equal to three. With these values the complete scheme converges in about 20 iterations.

5. Accuracy of the results

As pointed out above, the parameters of the inversion were chosen by trial and error for the specific data set considered. After these numerical tests, it appears that applying strong damping on source excitation and station response corrections warrant the stability and the convergence of the process. The Q model obtained when the process has converged to a minimum r.m.s. residue is weakly sensitive to the parameters of damping used, at least when the number of data is large enough. We will illustrate the importance of reaching a critical number of data by considering independent subsets of records of phase Lg1 at a frequency of 3 Hz. We performed the inversion with four different subsets of data. The numbers of sources of the four subsets used in the inversion are 25, 25, 55 and 100. In the case of the 25 earthquakes subsets, we reduced $N_{\min}$ to eight and $N_{S\min}$ to three, to cover an area similar to that of

the other cases. The Q models obtained are presented in Fig. 5. The result computed from the global data set is shown below in Fig. 7 (Lg1). The results obtained with the two subsets of 25 events are clearly in contradiction. In contrast, the main features of the Q distribution computed with the entire set of records are defined correctly when using only 55 or 100 earthquakes. We interpret this very strong dependence of the stability of the solution on the number of data by two characteristics of the technique of measurement used here. The first concerns the representation of the geometrical spreading term by a simple smooth functional dependence (eqn. (2)). This is an oversimplification even for synthetic Lg seismograms whose amplitudes exhibit large spatial fluctuations because of interferences, as shown by Campillo et al. (1984). The functional form of the spreading was defined by least squares over a large range of epicentral distance. The second point is that we assume azimuthal independence of both source excitation and site response, which results in poor precision of isolated attenuation measurements. These facts explain why the measurements, and therefore the inversion, reach statistical significance only for large data sets. In our first attempt to infer the attenuation in a limited part of France through a simple back-projection (Campillo, 1987), the number of events considered was too small. Nevertheless, even if some of the maps of Q were erroneous, the general conclusions of the study are confirmed by our new results, as will be shown below.

To add a control on the solution obtained for the entire data set, we constructed resolution maps computed as follows. Considering a model of Q_s,

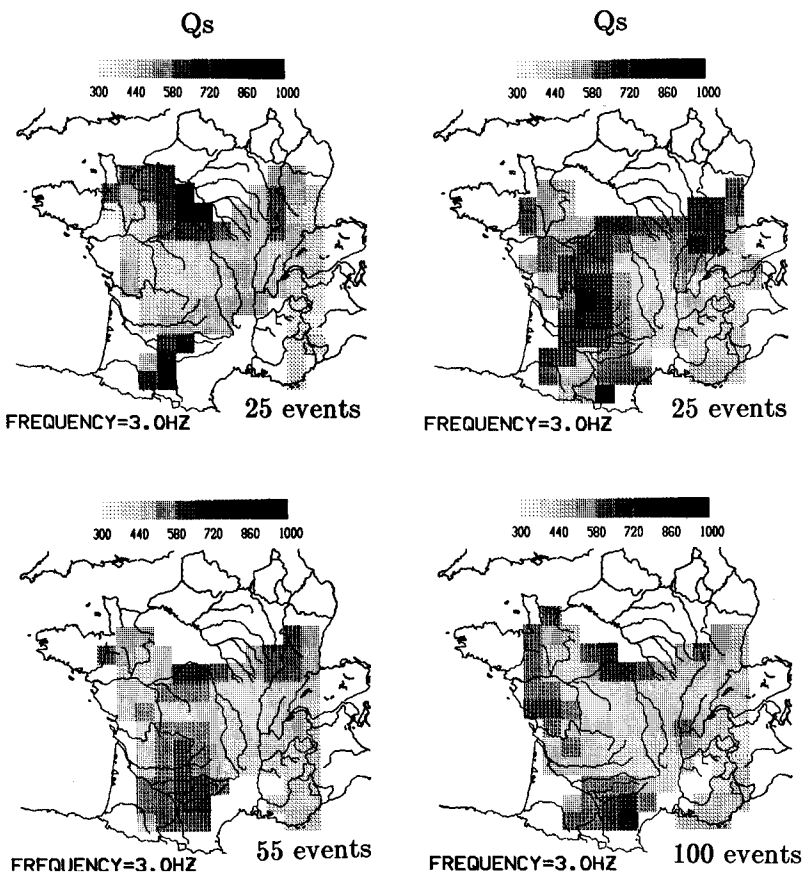

Fig. 5. Results obtained with different subsets of 25, 25, 55 and 100 events. The grid mesh is 60 km.

obtained are presented in Fig. 6 for six different locations. These maps give a critical view of our results; the perturbations are far from perfectly concentrated. Nevertheless, the perturbation occurs mostly in the region around the point considered, with very small effects in distant regions. This means that we can draw a relatively optimistic conclusion: our maps are very smoothed and therefore represent a long-wavelength image of the distribution of the quality factor, but, on the other hand, the inversion process does not produce strong spurious anomalies far from the region affected by the smoothing.

One may fear that a regional correlation of the station responses results in a strong trade-off with Q values. In practice, the stations are set up on firm ground sites and therefore, the local attenuation in the shallow layers is always weak compared with the attenuation along the whole path. The anomalies in the station responses are governed by resonances in the superficial layers, resulting in amplification in narrow frequency bands. The geometry of the shallow layers, and therefore the amplification at a given frequency, vary rapidly from place to place without significant regional correlation. This is confirmed by examination of the spectral site responses shown by Campillo et al. (1985), which are actually very close to our final results. The last point that we need to discuss for an objective presentation of our results is the misfit between observed and predicted values. Our main interest in this study is the mapping of Q_s. We have seen that to infer Q_s we also need to compute source excitation and station response. Considering these two last terms as a part of our model, we can compute directly from the actual spectral amplitude an apparent Q_s^{-1} value for each record that we compare with the value predicted by the heterogeneous Q model. All misfits due to source or stations are included in this comparison. The fact that we compute the misfits directly in terms of Q_s^{-1} allows us to compare the amplitude of the unresolved fluctuations of the data with the amplitude of the spatial variations of Q_s^{-1} obtained from our inversion. For a frequency of 3 Hz, we found in a model with homogeneous Q_s^{-1} a standard deviation of 8×10^{-4} for a mean Q_s^{-1} of 1.8×10^{-3}. After the inversion, the standard deviation is reduced to 4.5×10^{-4}. This indicates the significance of the quality factor fluctuations with respect to the average misfit of the data.

6. Results obtained at 3 Hz

We have performed the inversion for the four time windows defined previously at the same frequency of 3 Hz. The results obtained are presented in Fig. 7. The lowest Q values are reached for Q_p deduced from Pg waves. This result is somewhat surprising. As it is generally admitted that the values of intrinsic Q are larger for P waves than for S waves, another cause of apparent attenuation is required to understand this result. One possible explanation is that the Pg phase is more sensitive than the Lg phase to lateral large-scale heterogeneity in the crust. This can be explained by the fact that P waves incident on the Moho can always be refracted in the upper mantle, whereas S waves are trapped in the crust, for a wide range of incident angle. Nevertheless, as we will see later, considering the frequency dependence will lead us to invoke scattering in a randomly inhomogeneous medium to explain our results. The distribution of Q inferred from Pg does not exhibit strong variations at 3 Hz. The results obtained with the records corresponding to the window Lg1 are more contrasted. The zones of high attenuation correspond to the Alpine and peri-Alpine regions, the Central Massif and, more surprisingly, an area in the northwestern corner of the region studied that we will identify later as the Central Armorican Zone (see Fig. 1 for the locations of the regions). This example illustrates the difficulty of basing a regionalization of Q on surface geology only. We shall examine later the frequency dependence for Pg and Lg.

We also present in Fig. 7 the results obtained for the windows Lg2 and Lg3 that correspond to the early coda of Lg. We processed and inverted these data in exactly the same way as for Lg1, without taking into consideration the nature of their coda waves. For Lg2 the image presents a clear similarity with the results obtained with Lg1. The mean value of Q_s for Lg1 is slightly higher

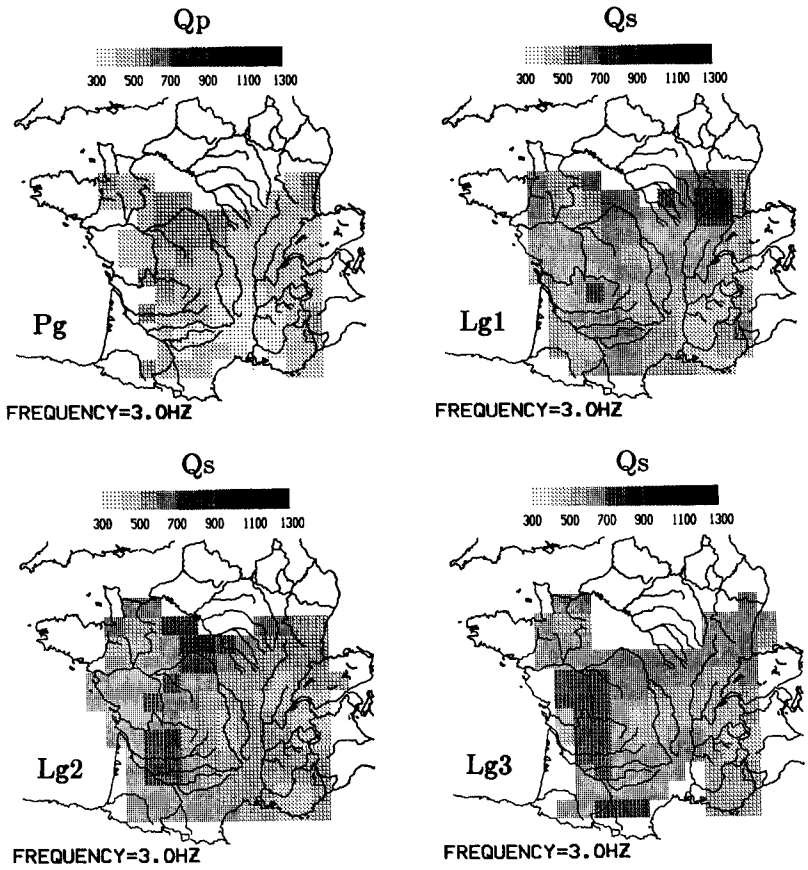

Fig. 7. Results obtained at 3 Hz for the four group velocity windows considered: Pg, Lg (Lg1), early coda of Lg (Lg2) and coda of Lg. All available records were used. The grid mesh is 60 km.

than that for Lg2. For Lg3 the image is poorly resolved, although one can distinguish features which are common to Lg1 and Lg2. The interpretation of the results obtained with late arrivals is difficult. Nevertheless, the very close average value of Q_s that we found from primary waves (Lg1) and from early coda (Lg2), assuming the same geometrical spreading for both phases, suggests that these waves are associated with a single mode of propagation, as discussed by Campillo (1990).

7. Frequency dependence of Q_s inferred from Lg1

Figure 8 presents the Q_s distributions computed at various frequencies. The images are less contrasted at high frequency, in addition to the fact that for high frequencies the contrast between quality factors with large values are much less significant in terms of energy attenuation. There are two different features for the patterns shown on the figure. First, some patterns have amplitudes that vary strongly with frequency and disappear almost completely at high frequency. This can be explained by the fact that the attenuation is dominated by the effect of scattering, which is known to result in a peak of attenuation in the frequency domain. The anomalous attenuation in the Central Armorican Zone is in this first category. Otherwise, the Alpine and peri-Alpine region seems to be associated with attenuation whatever the frequency is, although the contrast is more significant for the lowest frequencies. This point suggests the superimposition in this region

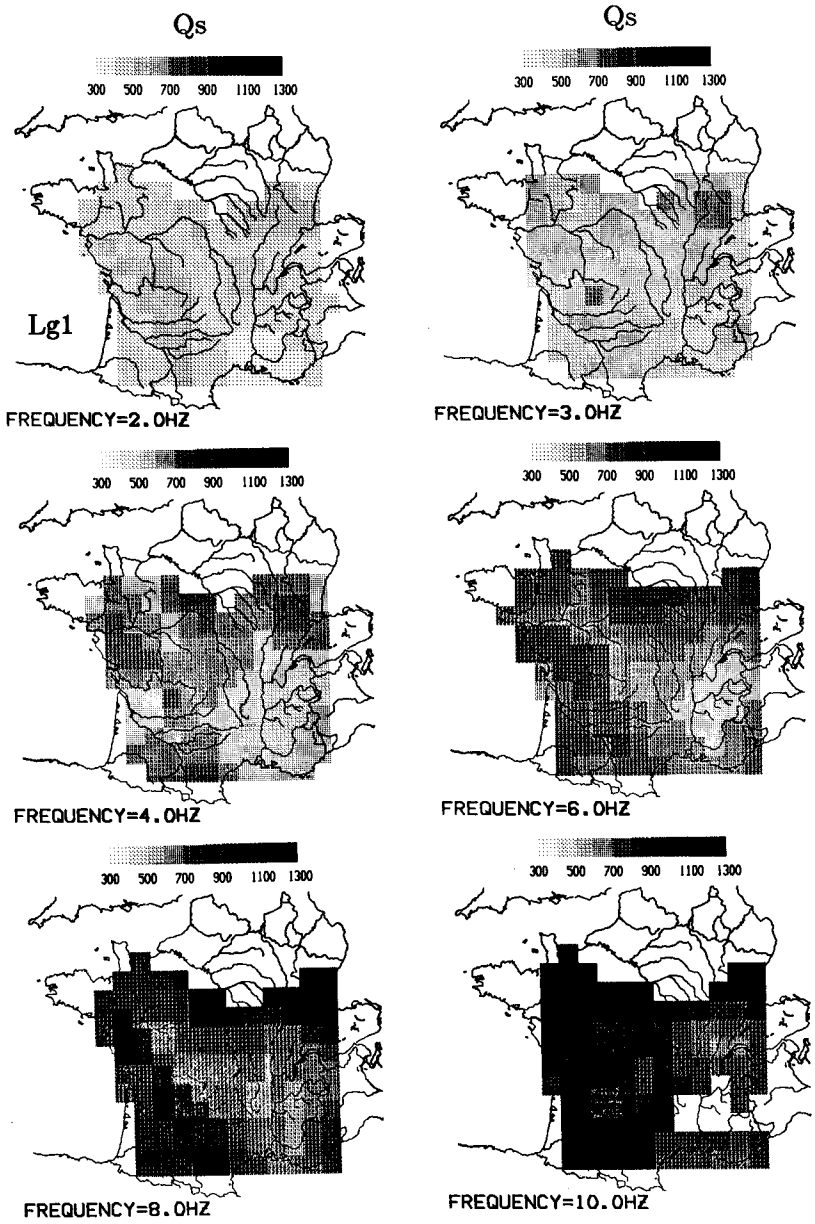

Fig. 8. Distribution of apparent attenuation of S wave in the crust obtained for the groups velocity window Lg1 for various frequencies. The mean values of Q_s obtained are the following: 459 (2 Hz), 589 (3 Hz), 689 (4 Hz), 720 (5 Hz), 792 (6 Hz), 922 (8 Hz) and 1020 (10 Hz). The grid mesh is 60 km.

of an important intrinsic frequency-independent attenuation on the scattering effect that dominates at low frequency. Indeed, there is a sedimentary basin as deep as 10 km at the western periphery of the Alpine arc. However, one cannot neglect the fact that a mountain range such as the Alps is associated with large-scale crustal heterogeneity. This can affect the geometrical spreading of Lg and result in apparent attenuation.

One conclusion that we can draw from these images is the clear frequency dependence of the mean quality factor and the decrease in amplitude

of the spatial variations of Q at high frequency. This was one of the main conclusions of an earlier study (Campillo, 1987) which aimed to show that apparent attenuation in the crust occurs in a limited frequency band. This result supports the hypothesis that attenuation of crustal waves is caused mainly by scattering on small-scale inhomogeneity rather than by factors that produce frequency-independent effects such as anelasticity or large-scale lateral heterogeneity. The distribution of Q follows the accepted trend that associates tectonically active regions with low Q. However, an intriguing problem is, for frequencies between 2 and 8 Hz, the existence of a region of high attenuation beneath the Hercynian basement of western France.

8. Frequency dependence of Q_p inferred from Pg

The results obtained for Q_p at four frequencies are presented in Fig. 9. The image obtained at 2 Hz is shown only to illustrate the strong frequency dependence of Q_p in this frequency range. In fact, Q_p varies with frequency even faster than does Q_s. There is a relatively good agreement between the patterns obtained for Q_p and Q_s, although the images obtained for Q_p are less contrasted. This

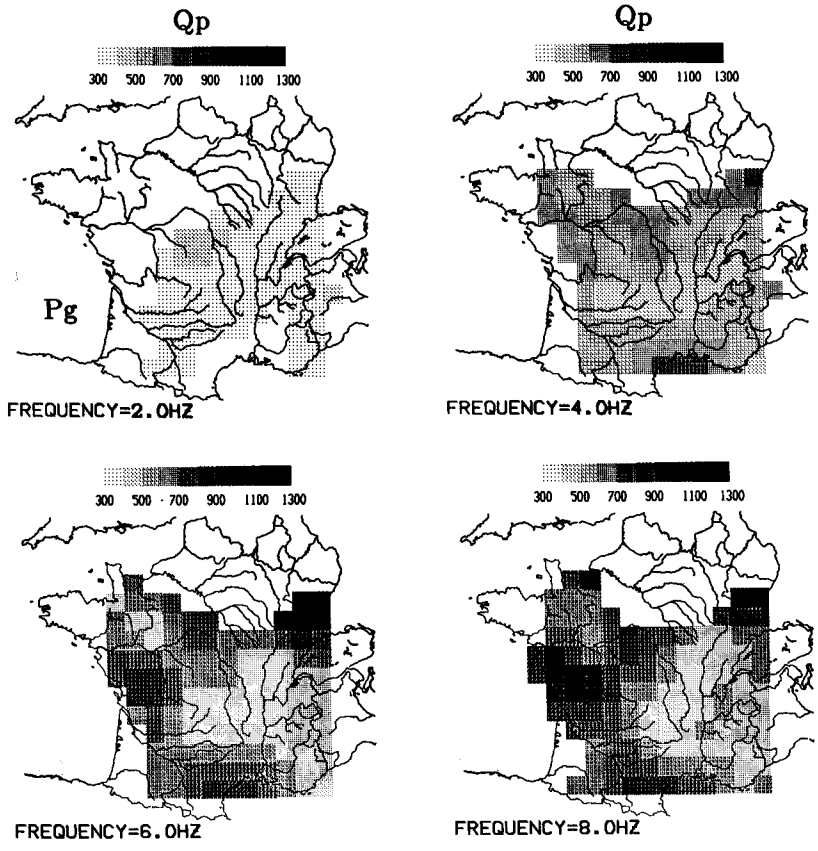

Fig. 9. Distribution of apparent attenuation of P wave in the crust computed from Pg waves. The mean values of Q_p are 310 at a frequency of 2 Hz, 550 at 4 Hz, 740 at 6 Hz and 800 at 8 Hz. The grid mesh is 60 km.

seems to indicate that, in spite of the different absolute values obtained for Q_s and Q_p, the causes of attenuation are the same for the two types of waves.

9. Discussion of the mean values of apparent Q_s

Q_p inferred from Pg is smaller than Q_s obtained from Lg1 over the whole frequency range. We can interpret both apparent attenuations in terms of intrinsic attenuation and scattering effect. If we consider the mean values of the quality factors, we find that the frequency dependence is stronger for Q_p than for Q_s. As this is also true for the different regions we will discuss only the results obtained for the mean values. This does not mean that the inversion is useless; on the contrary, it allows a better evaluation of source excitations and station responses and therefore a more accurate measurement of the mean value of Q.

The frequency dependence of the mean quality factors can be summarized by the following functional form:

$$\overline{Q}_p = 240 \times f^{0.6} \text{ and } \overline{Q}_s = 320 \times f^{0.5}$$

In an earlier study (Campillo et al., 1985), we found that $\overline{Q}_s = 290 \times f^{0.5}$, by assuming a homogeneous distribution of Q. The frequency dependence cannot be directly analyzed because anelasticity and scattering are both acting with a priori unknown strength. However, we can make reasonable assumptions about the frequency dependence of these two terms. Intrinsic Q has a high value with a very weak frequency dependence, as found from measurements in shield areas (Nuttli, 1982; Singh and Herrmann, 1983; Hasegawa, 1985). Sato (1984, 1990), under a single-scattering assumption, predicted that scattering Q varies with frequency for wavelengths smaller than the correlation distance. In these papers, Sato showed that his theoretical results are in agreement with observations made in various active regions. Assuming that we deal with wavelength smaller than the correlation distance, Sato's results indicate that the scattering Q is expected to be larger for S waves than for P waves, and this is effectively our observation. We have subtracted from our results

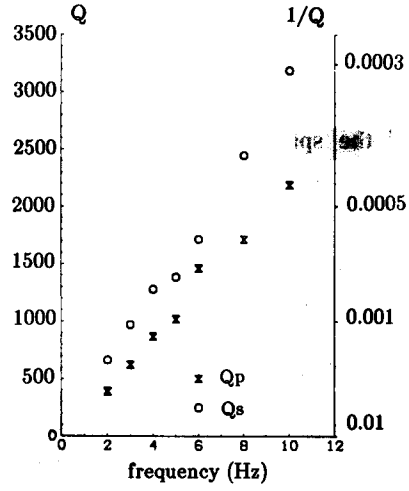

Fig. 10. Frequency dependence of the quality factor for P and S waves after correction of our results from a frequency-independent intrinsic Q of 1500.

the effect of the intrinsic attenuation that we consider to be represented by a constant Q of 1500. This corresponds to the value found by Nuttli (1982) for Q_s in a stable region, namely the central USA. We assume arbitrarily this same value for both P and S waves. After this correction we find Q_s^{scatt} and Q_p^{scatt} to be proportional to the frequency in the range 2–10 Hz, as shown in Fig. 10. The ratio between quality factors of S and P waves (about 1.5) is not as large as predicted by Sato (1984): 2.41. The ratio obtained here is dependent on our assumption about the value of anelastic Q. Nevertheless, as the observations at high frequency indicate that this value is at least 800, the ratio of Q_s^{scatt} to Q_p^{scatt} computed at low frequency is not very sensitive to our assumption about anelastic Q. If we assume a correlation distance of 2 km, our results indicate a mean fluctuation of 5% when measured from S waves and of 4% when measured from P waves. These values are actually very close. It should be remembered that this simple interpretation involves the assumption that the entire path of the wave is within the randomly inhomogeneous medium. These values can be underestimated if it appears that only a part of the crust is affected by the scattering. We can conclude from the mean values of the quality factor that there is a good agree-

ment between our experimental results and the theoretical predictions of Sato.

10. Discussion of the spatial distribution of apparent attenuation

We have discussed our results in terms of average values for the entire area and the whole depth of the crust. We may now try to understand the distribution of the apparent quality factor. One of the main features of our image is the attenuating character of the Alpine region. Nevertheless, we have seen that the poor resolution of our inversion in this area does not allow a detailed analysis of this very complex region. It is a well-known observation that active mountain ranges are associated with low Q. A more puzzling feature is the existence of a region of attenuating material elongated in a NW–SE direction in the northwestern part of France. This pattern is not correlated with the surface geology or the distribution of seismicity (Fig. 2 gives a realistic view of the seismicity). The direction of elongation corresponds to the structural direction of the Variscan basement in this region (Matte and Hirn, 1988). The deep crustal structures in this region have been known since the 'ECORS Nord de la France' experiment, which consisted of a vertical reflection seismic profile and a wide-angle profile (the latter is shown in Fig. 1). The records obtained with the latter technique have been interpreted by Matte and Hirn (1988). Their profile crosses the low-Q region that we found in northwestern

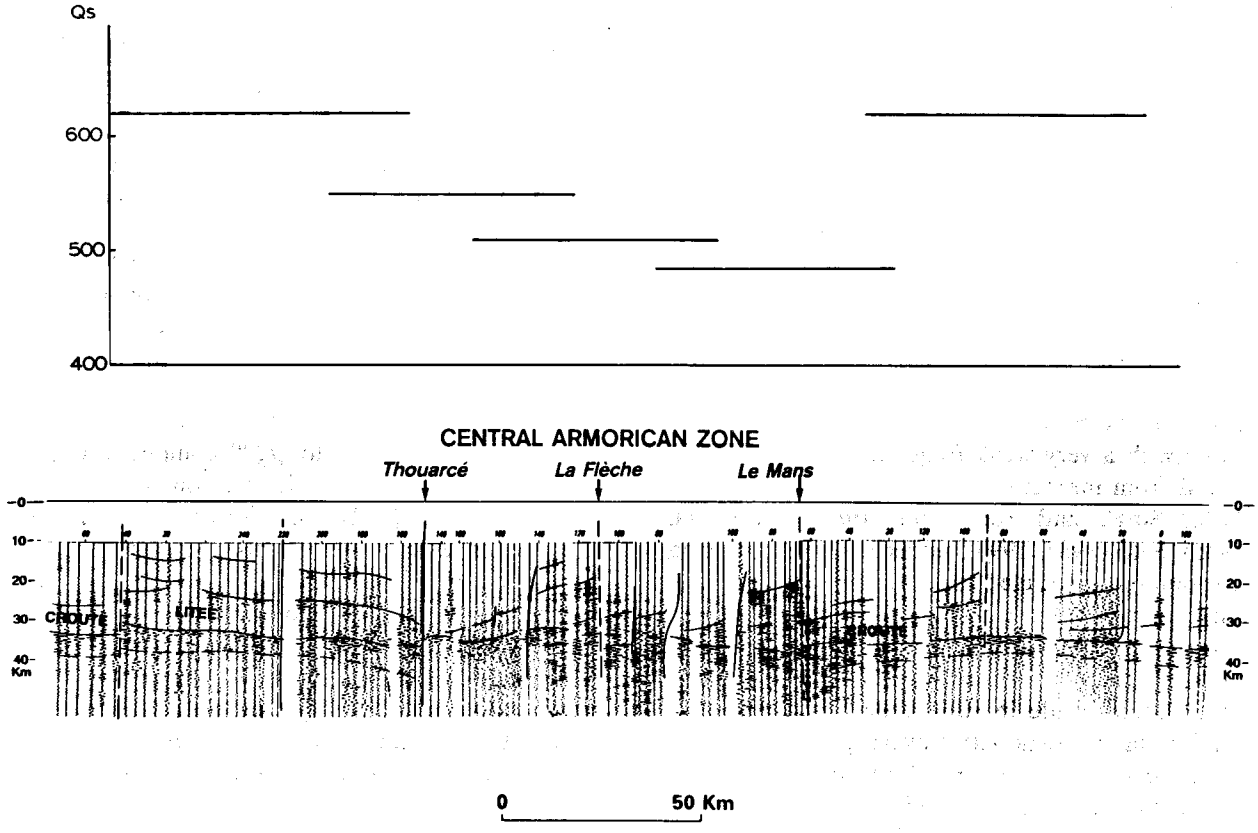

Fig. 11. Wide-angle reflection profile showing a zone of strong heterogeneity in the crust (after Matte and Hirn, 1988) and the apparent Q_s inferred from Lg (Lg1) at a frequency of 3 Hz.

France. This is a very fortunate opportunity to compare the apparent attenuation of the crust in a given region with its heterogeneity as revealed by seismic exploration. The part of the seismic section that corresponds to the intersection with the zone of higher attenuation is characterized by a very specific seismic signature, as shown in Fig. 11. This zone is bounded by two faults that seem to cross the entire crust (Matte and Hirn, 1988). The reflections from the lower crust are numerous and have large amplitudes, indicating strong impedance contrasts. This comparison between the image produced by the seismic reflection experiment and the apparent attenuation supports the hypothesis that scattering plays an important role in the attenuation of seismic waves within the crust. Indeed, this agreement may be fortuitous, but it is the only example of such a comparison that we can make with our data set.

An interesting feature of this comparison is that it indicates a correlation between the apparent attenuation of multiply reflected crustal waves and the heterogeneity of the lower crust. This heterogeneity is revealed by the large reflectivity in most of the examples of deep reflection profiles in Western Europe (e.g. Brown et al., 1986; Peddy and Hobbs, 1987). In contrast, the upper crust is generally more transparent to seismic waves. The strong scattering of short-period waves in the crust could be localized in the region of strong reflectivity, i.e. the lower crust. A controversial hypothesis could be drawn: most of the attenuation occurs in two regions of the crust: the first few kilometers beneath the surface, as suggested by Toksöz et al. (1988), and the highly inhomogeneous lower crust, as indicated in our example. The fact that a strong apparent attenuation and therefore an important scattering could occur in the possibly ductile lower crust is consistent with the framework proposed by Jin and Aki (1989) to explain temporal variations of coda Q.

11. Conclusion

We have shown that a precise measurement of Q_s or Q_p from regional phase records requires the processing of a large data set. The large trade-off between the unknowns necessitates a very careful interpretation of the results of the inversion. We believe that the inversion may also be useful to increase the accuracy of the measurement of the mean value of the quality factors. We have shown that the relatively poor resolution of our inversion results in an important smoothing of the image but does not produce artifacts.

The results obtained show the frequency dependence of Q_p and Q_s. A simple analysis shows that the mean values obtained are in agreement with the single-scattering model of Sato (1984), which implies a linear dependence of the quality factor on frequency, and larger values of Q_p than Q_s. We found that the mean fluctuation of velocity needed to explain the data is about 5%. The distribution of quality factors is governed by large-scale structures such as the Alpine range. We found that ancient structures can be associated with zones of high attenuation. The Central Armorican Zone in the Variscan belt is an example of that. Because we have an image of the crustal structure obtained by wide-angle reflection, we can associate the high apparent attenuation in this zone with scattering in a highly heterogeneous lower crust. Such a comparison between the apparent attenuation and the observed heterogeneity of the crust must be repeated elsewhere to confirm the correlation obtained in this paper. Quality factor tomography is useful for the quantitative interpretation of short-period seismic phases, but if such a correlation is confirmed it could also be a promising tool for investigation of deep crustal structures.

Acknowledgements

We thank M. Ukawa, M. Bouchon and F.J. Sanchez-Sesma for their useful comments.

References

Aki, K., 1969. Analysis of the seismic coda of local earthquakes as scattered waves. J. Geophys. Res., 74: 615–631.

Brown, L., Barazangi, M., Kaufman, S. and Oliver, J., 1986. The first decade of COCORP 1974–1984. In: M. Barazangi

and L. Brown (Editors), Reflection Seismology: A Global Perspective. Am. Geophys. Union Geodyn. Series, 13: 107–120.

Campillo, M., 1987. Lg wave propagation in a laterally varying crust and the distribution of quality factor in Central France. J. Geophys. Res., 92: 12604–12614.

Campillo, M., 1990. Propagation and attenuation characteristics of the crustal phase Lg. Pure Appl. Geophys., 132: 1–19.

Campillo, M., Bouchon, M. and Massinon, B., 1984. Theoretical study of the excitation, spectral characteristics and geometrical attenuation of regional seismic phases. Bull. Seismol. Soc. Am., 74: 79–90.

Campillo, M., Plantet, J.L. and Bouchon, M., 1985. Frequency dependent attenuation in the crust beneath Central France from Lg waves: data analysis and numerical modelling. Bull. Seismol. Soc. Am., 75: 1395–1411.

Cote, P., 1988. Tomographies sismiques en génie civil. Ph.D. Thesis, Université Joseph Fourier, Grenoble.

Gilbert, P., 1972. Iterative methods for the three dimensional reconstruction of an object from projections. J. Theor. Biol., 36: 105–117.

Gupta, I.N., McLaughlin, K.L., Wagner, R.A., Jih, R.S. and McElfresh, T.W., 1989. Seismic wave attenuation in eastern North America. EPRI RP 2556-9 final report. EPRI, Palo Alto, CA.

Hasegawa, H.S., 1985. Attenuation of Lg waves in the Canadian shield. Bull. Seismol. Soc. Am., 75: 1569–1582.

Herraiz, M. and Espinoza, A.F., 1987. Scattering and attenuation of high frequency seismic waves: development of the theory of coda waves. Pure Appl. Geophys., 125: 499–577.

Jin, A. and Aki, K., 1989. Spatial and temporal correlation between coda Q^{-1} and seismicity and its physical mechanism. J. Geophys. Res., 94: 14041–14059.

Johnston, D.H., 1981. Attenuation: a state-of-the-art summary. In: M.N. Toksöz and D.H. Johnston (Editors), Geophysics Reprint Series No. 2, Society of Exploration Geophysics.

Kennett, B.L.N., 1984. Guided wave propagation in laterally varying media, I, Theoretical development. Geophys. J.R. Astron. Soc., 79: 235–255.

Mason, I.M., 1981. Algebraic reconstruction of two-dimensional velocity inhomogeneity in the High Hazles seam of Thoresby colliery. Geophysics, 46: 298–308.

Matte, P. and Hirn, A., 1988. Seismic signature and tectonic cross section of the Variscan crust. Tectonics, 7: 141–155.

Maupin, V., 1989. Numerical modelling of Lg propagation across the North Sea central graben. Geophys. J. Int., 99: 273–283.

Nicolas, M, Massinon, B., Mechler, P. and Bouchon, M., 1982. Attenuation of regional phases in Western Europe. Bull. Seismol. Soc. Am., 72: 2089–2106.

Nuttli, O., 1973. Seismic wave attenuation and magnitude relations for eastern North America. J. Geophys. Res., 78: 876–885.

Nuttli, O., 1982. The earthquake problem in the eastern United States, J. Struct. Div. Am. Soc. Civ. Eng., 108: 1302–1312.

Nuttli, O., 1986. Yield estimates of Nevada Test Site explosions obtained from seismic Lg waves. J. Geophys. Res., 91: 2137–2151.

Peddy, C.P. and Hobbs, R.W., 1987. Lower crustal reflectivity of the continental margin Southwest of Britain. Ann. Geophys., B5: 331–338.

Sato, H., 1984. Attenuation and envelope formation of three-component seismograms of small local earthquakes in randomly inhomogeneous lithosphere. J. Geophys. Res., 89: 1221–1241.

Sato, H., 1990. Unified approach to amplitude attenuation and coda excitation in the randomly inhomogeneous lithosphere. Pure Appl. Geophys., 132: 93–121.

Singh, S.K. and Herrmann, R.B., 1983. Regionalization of crustal coda Q in the continental United States. J. Geophys. Res., 88: 527–538.

Toksöz, M.N., Dainty, A., Reuter, E., and Wu, R.S., 1988. A model for attenuation and scattering in the Earth's crust. Pure Appl. Geophys., 128: 81–101.

Wang, C.Y. and Herrmann, R.B., 1988. Synthesis of coda waves in layered medium. Pure Appl. Geophys., 128: 7–42.

Zeng, Y.H., Faulkner, J., Teng, T.L. and Aki, K., 1987. Focusing and defocusing of Rayleigh waves from USSR across arctic region to US. EOS Trans. Am. Geophys. Union, 68: 1377.